The DIA-Method for Navigational Integrity

P.J.G. Teunissen[1,2]
[1] *Delft University of Technology, Delft, The Netherlands*
[2] *Curtin University, Perth, Australia*

ABSTRACT: In this contribution we present a review of the DIA-method to ensure navigational integrity. The DIA-method rigorously combines parameter estimation and statistical testing for the Detection, Identification and Adaptation of multivariate and multiple model misspecifications. We describe the statistical properties of the so-obtained DIA-estimator together with its probability density function. Numerical examples are given to highlight various aspects of the navigational DIA-estimator.

1 INTRODUCTION

Parameter estimation and statistical testing are crucial components in any navigational data processing system. The DIA method for the Detection, Identification and Adaptation of model misspecifications combines estimation with testing. Parameter estimation is conducted to determine estimates for the parameters of interest and statistical testing is conducted to validate the results with the aim of removing any unwanted biases that may be present. In order to rigorously capture the estimation-testing combination, the DIA-estimator has been introduced in [1], together with a unifying probabilistic framework. This allows one to take into account the intricacies of the combination when evaluating the contributions of the decisions and estimators involved. As it will be shown, this inclusion of the estimation+testing combination is crucial to be able to obtain a rigorous quality and integrity-risk description of one's position and navigational results. Such rigor is needed so as to avoid too optimistic, and therefore dangerous, navigational integrity assessments.

2 THE DIA-METHOD

A brief review is given of the Detection-Identification-Adaptation (DIA) method. Although the method is applicable for any statistical identification procedure, we here use for illustration purposes the relatively simple datasnooping procedure for single-outlier identification [1].

2.1 *Statistical Hypotheses*

We first formulate the null- and alternative hypotheses, denoted by H_0 and H_i, respectively. As alternative hypotheses, we consider those describing outliers in individual observations. Here we restrict ourselves to the case of one outlier at a time. In that case there are as many alternative hypotheses as there are observations. Therefore, the observational model under H_0 and H_i is given as

$$H_0: \quad E(y) = A\,x; \quad D(y) = Q_{yy} \tag{1}$$

$$H_i: \quad E(y) = A\,x + c_i b_i; \quad D(y) = Q_{yy} \tag{2}$$

with $E(\cdot)$ the expectation operator, $D(\cdot)$ the dispersion operator, $y \in \mathbb{R}^m$ the normally distributed random vector of observables linked to the estimable unknown parameters through the design matrix $A \in \mathbb{R}^{m \times n}$ of $\text{rank}(A) = n$, and $Q_{yy} \in \mathbb{R}^{m \times m}$ the positive-definite variance matrix of y. The redundancy of H_0 is $r = m - \text{rank}(A) = m - n$. c_i is the canonical unit vector having one as its ith entry and zeros elsewhere, and b_i is the scalar bias. Note that $[A \;\; c_i]$ is a known matrix of full rank. As the number of observations is equal to m, there are also m alternative hypotheses H_i defined in (2); $i = 1,\ldots,m$.

The best linear unbiased estimator (BLUE) of the unknown parameters x is given by

$$\text{H}_0: \quad \hat{x}_0 = A^+ y \qquad \text{H}_{i \neq 0}: \quad \hat{x}_i = \overline{A}_i^+ y \tag{3}$$

with $A^+ = (A^T Q_{yy}^{-1} A)^{-1} A^T Q_{yy}^{-1}$ the BLUE-inverse of A, $\overline{A}_i^+ = (\overline{A}_i^T Q_{yy}^{-1} \overline{A}_i)^{-1} \overline{A}_i^T Q_{yy}^{-1}$ the BLUE-inverse of $\overline{A}_i = P_{c_i}^\perp A$ and $P_{c_i}^\perp = I_m - c_i (c_i^T Q_{yy}^{-1} c_i)^{-1} c_i^T Q_{yy}^{-1}$ being an orthogonal projector that projects onto the orthogonal complement of the range space of c_i.

2.2 *DIA-datasnooping procedure*

The DIA-method has been widely employed in a variety of applications, such as the quality control of positioning and navigation, and the integrity monitoring of GNSS models, see e.g. [2, 3]. The DIA steps are realized using the *misclosure* vector $t \in \mathbb{R}^r$ given as

$$t = B^T y; \qquad Q_{tt} = B^T Q_{yy} B \tag{4}$$

where the $m \times r$ matrix B is a full-rank matrix, with $\text{rank}(B) = r$, of which the range space is an orthogonal complement of that of A, i.e. $[A \;\; B] \in \mathbb{R}^{m \times m}$ is invertible and $A^T B = 0$. With $y \sim \text{N}(Ax + c_i b_i, Q_{yy})$ for $i = 0,1,\ldots,m$ and $c_0 b_0 = 0$, the misclosure vector is then distributed as

$$t \overset{\text{H}_i}{\sim} \text{N}(\mu_{t_i} = B^T c_i b_i, Q_{yy}) \qquad \text{for} \;\; i = 0,1,\ldots,m \tag{5}$$

As t is zero-mean under H_0 and also independent of $\hat{x}_0$, it provides all the available information useful for validation of H_0 [1]. Thus, an unambiguous testing procedure can be established through assigning the outcomes of t to the statistical hypotheses H_i for $i = 0,1,\ldots,m$.

The DIA-datasnooping procedure is specified as follows:

1. *Detection*: Accept H_0 if $t \in \text{P}_0$ with

$$\text{P}_0 = \left\{ t \in \mathbb{R}^r \,\middle|\, ||t||_{Q_{tt}}^2 \leq k_{\alpha,r} \right\} \tag{6}$$

in which $||\cdot||_{Q_{tt}}^2 = (\cdot)^T Q_{tt}^{-1} (\cdot)$ and $k_{\alpha,r}$ is the $\alpha-$percentage of the central Chi-square distribution with r degrees of freedom. If H_0 is accepted, then

$\hat{x}_0$ is provided as the estimate of x. Otherwise, go to step 2.

2. *Identification*: Compute Baarda's test statistic for all alternative hypotheses as [4, 5]

$$w_i = \frac{c_{t_i}^T Q_{tt}^{-1} t}{\sqrt{c_{t_i}^T Q_{tt}^{-1} c_{t_i}}} \tag{7}$$

in which $c_{t_i} = B^T c_i$ is the ith column of matrix B^T since c_i is a canonical unit vector. Select $\text{H}_{i \neq 0}$ if $t \in \text{P}_{i \neq 0}$ with

$$\text{P}_{i \neq 0} = \left\{ t \in \mathbb{R}^r / \text{P}_0 \,\middle|\, |w_i| = \max_{j \in \{1,\ldots,m\}} |w_j| \right\} \tag{8}$$

3. *Adaptation*: When H_i is selected, then $\hat{x}_i$ is provided as the estimate of x.

The partitioning P_i in terms of the (original) misclosure vector is introduced in [1], and an example is shown in Figure 3 in [ibid].

3   THE DIA-ESTIMATOR

Given the above three steps, estimation and testing are *combined* in DIA-datasnooping. A unifying framework is presented in [1] to rigorously capture the probabilistic properties of this combination.
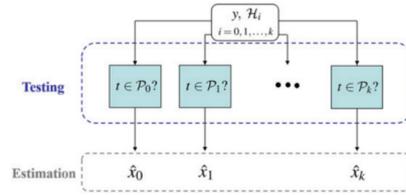
Figure 1. Estimation and testing combined leads to the DIA-estimator [6].

As such, the *DIA-estimator* $\overline{x}$ was introduced, which captures the whole estimation-testing scheme and it is given as (see Figure 1)

$$\overline{x} = \sum_{j=0}^{m} \hat{x}_j \, p_j(t) \tag{9}$$

with $p_j(t)$ being the indicator function of region P_j, i.e. $p_j(t) = 1$ for $t \in \text{P}_j$ and $p_j(t) = 0$ elsewhere. Therefore, the DIA-estimator $\overline{x}$ is a combination of $\hat{x}_j$ for $j = 0,1,\ldots,m$ and the misclosure vector t. The Probability Density Function (PDF) of $\overline{x}$ under H_i reads [1]

$$\begin{aligned} f_{\overline{x}}(\theta \,|\, \text{H}_i) &= \sum_{j=0}^{m} \int_{\text{P}_j} f_{\hat{x}_j, t}(\theta, \tau \,|\, \text{H}_i) \, d\tau \\ &= \sum_{j=0}^{m} \int_{\text{P}_j} f_{\hat{x}_0}(\theta + L_j \tau \,|\, \text{H}_i) f_t(\tau \,|\, \text{H}_i) \, d\tau \end{aligned} \tag{10}$$

where the second equality is a consequence of

$$\hat{x}_j = \hat{x}_0 - L_j\, t \tag{11}$$

with

$$L_j = \frac{1}{\|c_{t_j}\|^2_{Q_{tt}}} A^+ c_j c_{t_j}^T Q_{tt}^{-1} \tag{12}$$

It is important to realize, although we are working with linear models (cf. 1 and 2) and linear estimators $\hat{x}_j$ based normally distributed data, that the DIA-estimator $\bar{x}$, which captures the final outcome of our combined estimation+testing process, is now *not* normally distributed anymore. Its distribution is given by (10) and it is this expression that one needs to use when evaluating the quality or integrity risks of one's positioning or navigational results.

4 THE DIA-ESTIMATOR IN CASE OF A SINGLE ALTERNATIVE HYPOTHESIS

To illustrate the characteristics of the DIA-estimator, we take the single alternative hypothesis case as a simple example. Suppose that in (1), there is only one unknown parameter ($n = 1$) and also the redundancy of the model is one ($r = 1$), i.e. $x \in \mathbb{R}$ and $t \in \mathbb{R}$. The canonical form of such a model, applying the Tienstra-transformation T to the normally distributed vector of observables y [1], reads

$$\mathsf{T}\, y = \begin{bmatrix} A^+ \\ B^T \end{bmatrix} y = \begin{bmatrix} \hat{x}_0 \\ t \end{bmatrix} \overset{\mathsf{H}_i}{\sim} \mathrm{N}\left(\begin{bmatrix} x + b_{\hat{x}_{0,i}} \\ b_{t_i} \end{bmatrix}, \begin{bmatrix} \sigma^2_{\hat{x}_0} & 0 \\ 0 & \sigma^2_t \end{bmatrix} \right) \tag{13}$$

which is specified for $i \in \{0, a\}$ as

$$\begin{aligned} \mathsf{H}_0 &:\quad b_{\hat{x}_{0,0}} = 0, \qquad b_{t_0} = 0 \\ \mathsf{H}_a &:\quad b_{\hat{x}_{0,a}} = L_a b_a, \quad b_{t_a} = b_a \end{aligned} \tag{14}$$

for some $b_a \in \mathbb{R}/\{0\}$, and also $L_a \in \mathbb{R}$ which establishes the following link

$$\hat{x}_a = \hat{x}_0 - L_a t \tag{15}$$

so that $E(\hat{x}_a | \mathsf{H}_0) = E(\hat{x}_a | \mathsf{H}_a) = x$.

The corresponding DIA-datasnooping procedure is then defined as:
1. *Detection*: Accept H_0 if $t \in \mathsf{P}_0$ with

$$\mathsf{P}_0 = [-\sqrt{k_{\alpha,1}}\,,\ \sqrt{k_{\alpha,1}}] \tag{16}$$

Provide $\hat{x}_0$ as the estimate of x.
2. *Identification*: Select H_a if $t \in \mathsf{P}_0^c$ with $\mathsf{P}_0^c = \mathbb{R}/\mathsf{P}_0$.
3. *Adaptation*: When H_a is selected, $\hat{x}_a$ is provided as the estimate of x.

With the above three steps, the DIA-estimator and its PDF under H_i, $i \in \{0, a\}$, are given by

$$\bar{x} = \hat{x}_0\, p_0(t) + \hat{x}_a\, (1 - p_0(t)) \tag{17}$$

and

$$\begin{aligned} f_{\bar{x}}(\theta | \mathsf{H}_i) &= f_{\hat{x}_0}(\theta | \mathsf{H}_i) + \\ &+ \int_{\mathsf{P}_0^c} \left[f_{\hat{x}_0}(\theta + L_a \tau | \mathsf{H}_i) - f_{\hat{x}_0}(\theta | \mathsf{H}_i) \right] f_t(\tau | \mathsf{H}_i)\, d\tau \end{aligned} \tag{18}$$

As there is only one alternative hypothesis H_a, there are four events to consider: Correct Acceptance (CA), False Alarm (FA), Missed Detection (MD) and Correct Detection (CD). Using their probability of occurrences, the PDF of the DIA-estimator $f_{\bar{x}}(\theta | \mathsf{H}_i)$ can be decomposed as

$$\begin{aligned} f_{\bar{x}}(\theta | \mathsf{H}_0) &= f_{\hat{x}_0}(\theta | \mathsf{H}_0)\, \mathrm{P_{CA}} + f_{\hat{x}_a|\mathrm{FA}}(\theta | \mathrm{FA})\, \mathrm{P_{FA}} \\ f_{\bar{x}}(\theta | \mathsf{H}_a) &= f_{\hat{x}_0}(\theta | \mathsf{H}_a)\, \mathrm{P_{MD}} + f_{\hat{x}_a|\mathrm{CD}}(\theta | \mathrm{CD})\, \mathrm{P_{CD}} \end{aligned} \tag{19}$$

In Figure 2, considering $\sigma^2_{\hat{x}_0} = 0.5\mathrm{m}^2$, $\sigma^2_t = 2\mathrm{m}^2$ and $L_a = 0.5$, we show how the PDFs $f_{\bar{x}}(\theta | \mathsf{H}_0)$ [top] and $f_{\bar{x}}(\theta | \mathsf{H}_a)$ [middle and bottom] are formed according to (19). The solid and dashed *blue* curves, respectively, depict $f_{\hat{x}_0}(\theta | \mathsf{H}_0) = f_{\bar{x}|\mathrm{CA}}(\theta | \mathrm{CA})$ and $f_{\hat{x}_a|\mathrm{FA}}(\theta | \mathrm{FA})$ in the top panel, and $f_{\hat{x}_0}(\theta | \mathsf{H}_a) = f_{\bar{x}|\mathrm{MD}}(\theta | \mathrm{MD})$ and $f_{\hat{x}_a|\mathrm{CD}}(\theta | \mathrm{CD})$ in the middle and bottom panels. The *black* curve shows $f_{\hat{x}_a}(\theta | \mathsf{H}_0)$ which is also equal to $f_{\hat{x}_a}(\theta | \mathsf{H}_a)$.

These results clearly show how the PDF of the DIA-estimator differs from the PDFs of $\hat{x}_0$ and $\hat{x}_a$.

5 DIA CONFIDENCE REGION IN CASE OF MULTIPLE ALTERNATIVE HYPOTHSES

So far, we have been working with an observational model with one unknown parameter and one redundancy. In this section, we work with the satellite-based single point positioning (SPP) model based on the observations of m satellites with four unknown parameters ($n = 4$) and $r = m - 4$ redundancy. As alternative hypotheses, we consider those given in (2). In that case there are as many alternative hypotheses as there are observations.

Assuming there are m pseudorange observations, the observational model under H_i for $i = 0, 1, \ldots, m$ is given as

$$\mathsf{H}_i:\quad E(y) = [G \quad e_m] \begin{bmatrix} x \\ dt \end{bmatrix} + c_i b_i\ ,\quad Q_{yy} = \sigma^2_p I_m \tag{20}$$

where the $m \times 3$ matrix $G = [-u_1^T, \ldots, -u_m^T]^T$ contains the receiver-satellite unit direction vectors u_i as its rows, and e_m is the m − vector of ones, and again with $c_0 b_0 = 0$. The unknown receiver coordinate components and clock error are, respectively, denoted by the 3-vector x and scalar dt. The dispersion of the observables is characterized through the standard deviation σ_p and the identity matrix I_m. At this stage, in order to simplify our analysis, we do not consider a satellite elevation-dependent variance matrix.
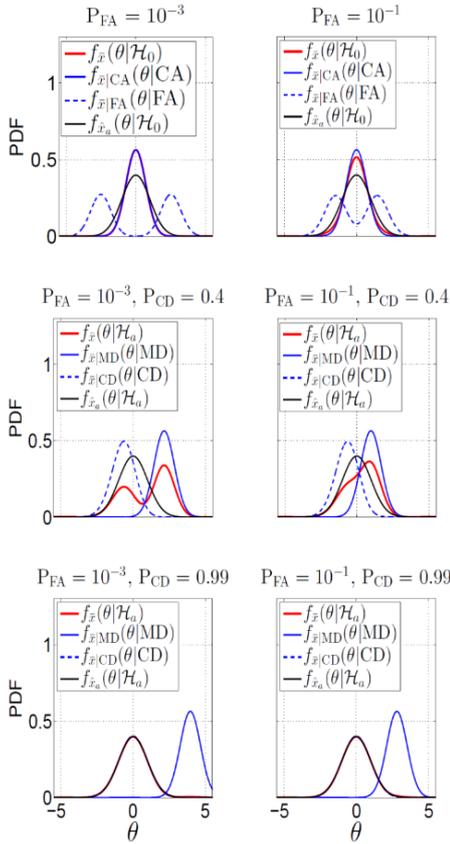
Figure 2. Illustration of the DIA-estimator PDF [top] under null hypothesis $\mathcal{H}_0$ and [middle and bottom] under alternative hypothesis $\mathcal{H}_a$. The contributing parameters are set as $\sigma_{\hat{x}_0}^2 = 0.5\text{m}^2$, $\sigma_t^2 = 2\text{m}^2$, $L_a = 0.5$. Panels, from left to right, correspond to $\text{P}_{\text{FA}} = 10^{-3}$ and $\text{P}_{\text{FA}} = 10^{-1}$. Panels in the middle and at the bottom correspond to resp. $\text{P}_{\text{CD}} = 0.4$ and $\text{P}_{\text{CD}} = 0.99$.

For integrity purposes, it is common to describe the quality of an estimator of x by computing its corresponding confidence region or confidence level [7]. To construct the confidence region for the parameters of interest, one may define beforehand the shape of the region, for example, spherical, ellipsoidal, or rectangular, and then compute its size for a given confidence level [8, 9], or have the confidence region determined by the contours of the PDF of the estimator for a given confidence level [10, 11]. Whichever approach is taken, the properties of the confidence region are determined by the probabilistic properties of the estimator. It is therefore crucial, in order to have a realistic confidence region, that one works with the correct PDF of one's estimator. This implies, when exercising a DIA procedure, one should use the PDF of the DIA estimator $\bar{x}$ rather than the PDF of its constituent estimators $\hat{x}_i$. To emphasize this, we compare three different confidence regions under null-hypothesis as follows:

1. An *ellipsoidal* 100(1-α)% confidence region *E(x)* based on the normal distribution of $\hat{x}_0$ under $\mathcal{H}_0$. This is the region that one normally uses in practice for constructing a confidence region. Note however, that this region neglects the probabilistic impact of testing.
2. An *ellipsoidal* 100(1-α)% confidence region *E′(x)*, that has the same shape as *E(x)*, but with a size determined by the nonnormal PDF of the DIA-estimator under the null-hypothesis.
3. A 100(1-α)% confidence region *C(x)* of which the shape and size are determined as the *highest density*

region [10, 11] of the nonnormal PDF of the DIA-estimator under the null-hypothesis.

Figure 3 shows the above three confidence regions for the SPP model (20) corresponding with the Figure 4 skyplot. The larger size of the red ellipse comparing to the blue one demonstrates that the confidence region *E(x)* has a poor coverage in the sense that it provides a *too optimistic* picture and that it should thus be made larger in order to contain the required probability of the DIA estimator. It will be clear that a too optimistic assessment is dangerous in case of safety-of-life applications. The green region *C(x)* in Fig. 4 is significantly different in shape from the ellipsoidal confidence region which is conventionally used. Depending on the α value, *C(x)* can be a nonconvex region, which is caused by the shape of the nonnormal PDF of the DIA-estimattor under the null-hypothesis. This shows again the influence testing has on confidence-statements and that one therefore should use the PDF of the DIA-estimator to evaluate the quality of estimated position and navigation results.
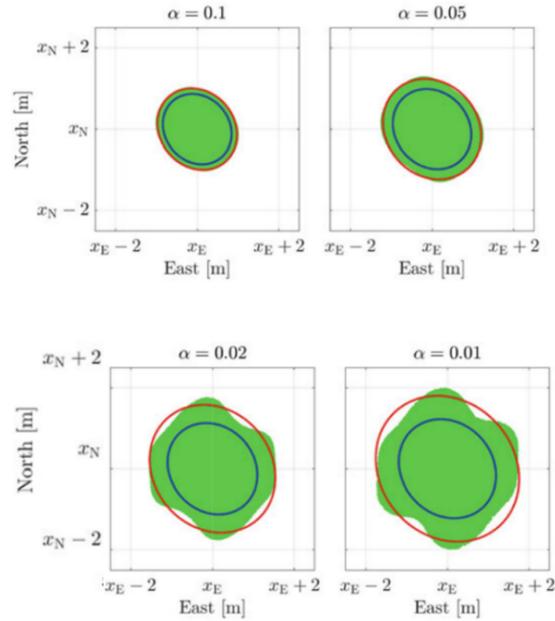

Figure 3. Illustration of 100(1-α)% confidence regions for the SPP model (20) corresponding with the skyplot of Fig 4. The results show different values of α, with σ_p=0.5m and P_{FA}=0.1. In each panel, green area indicates the region *C(x)*, red ellipse indicates boundary of *E′(x)* and blue ellipse indicates the boundary of *E(x)* [6].
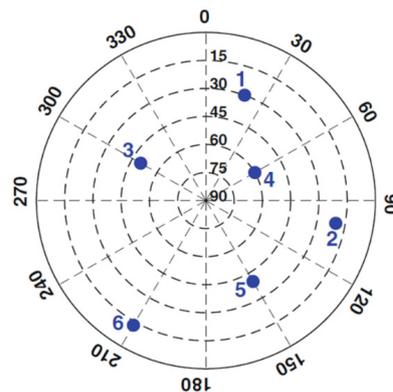

Figure 4: Skyplot of six satellites.

6 SUMMARY AND CONCLUSION

The message of this contribution finds its origin in the combination of parameter estimation and statistical testing. These two activities are typically disconnected in practice, when it comes to describing the quality of the eventual estimator. That is, the distribution of the estimator under an identified alternative hypothesis is usually used, without regard to the conditioning process that led to the decision to accept this hypothesis as the working model. We analysed what the contribution of this negligence is to the actual integrity risk and showed that for a rigorous assessment one should use the DIA-estimator and its probability density function.

REFERENCES

[1] Teunissen PJG (2017) Distributional theory for the DIA method. Journal of Geodesy, Springer, 1–22, DOI 10.1007/s00190-017-1045-7.

[2] Teunissen PJG (1990) An integrity and quality control procedure for use in multi-sensor integration. In: Proc. of ION GPS-1990, ION, pp 513–522

[3] Amiri Simkooei A (2001) Comparison of reliability and geometrical strength criteria in geodetic networks. Journal of Geodesy 75(4):227–233

[4] Baarda W (1967) Statistical concepts in geodesy. Netherlands Geodetic Commission, Publ. on geodesy, New series 2(4)

[5] Teunissen PJG (2000) Testing theory: an introduction. Delft University Press, Series on Mathematical Geodesy and Positioning

[6] Zaminpardaz S, Teunissen PJG (2022): GNSS Detection and Estimation. Encyclopedia of Geodesy, Springer, MG Sideris (Ed.), 1-9.

[7] Koch KR (1999): Parameter estimation and hypothesis testing in linear models. Springer Science & Business Media.

[8] Hoover W (1984): Algorithms for confidence circles and ellipses (NOAA Technical Report NOS 107 C&GS 3). Rockville, MD: National Oceanic and Atmospheric Administration.

[9] Hofmann-Wellenhof B, Legat K, Wieser M (2003): Navigation: Principles of Positioning and Guidance. Springer.

[10] Hyndman RJ (1996): Computing and graphing highest density regions. The American Statistician 50(2): 120 - 126.

[11] Teunissen PJG (2007): Least-squares prediction in linear models with integer unknowns. Journal of Geodesy 81: 565-579.